Suppression of core polarization in halo nuclei

T.T.S. Kuo[1], F. Krmpotić[2], and Y. Tzeng[3]

[1] *Department of Physics, SUNY-Stony Brook*

Stony Brook, New York 11794 USA

[2] *Departamento de Física, Facultad de Ciencias Exactas*

Universidad Nacional de La Plata, C. C. 67, 1900 La Plata, Argentina

[3] *Institute of Physics, Academia Sinica*

Nankang, Taipei, Taiwan

(February 9, 2008)

Abstract

We present a microscopic study of halo nuclei, starting from the Paris and Bonn potentials and employing a two-frequency shell model approach. It is found that the core-polarization effect is dramatically suppressed in such nuclei. Consequently the effective interaction for halo nucleons is almost entirely given by the bare G-matrix alone, which presently can be evaluated with a high degree of accuracy. The experimental pairing energies between the two halo neutrons in ^6He and ^{11}Li nuclei are satisfactorily reproduced by our calculation. It is suggested that the fundamental nucleon-nucleon interaction can be probed in a clearer and more direct way in halo nuclei than in ordinary nuclei.

PACS numbers: 21.30.+y,21.60.Cs, 21.90.+f

Radioactive-beam nuclear physics has been progressing rapidly, and there is much current interest in studying halo nuclei [1,2]. There were four articles about halo nuclei in a recent issue of Physical Review C: Nazarewicz *et al.* [3] dealt with the halo nuclei around the nucleus ^{48}Ni, Hamamoto *et al.* [4] carried out a systematic investigation of the single particle and collective degrees of freedom in the drip-line nuclei, and an experimental study of heavy halo nuclei around $N = 82$ was also presented [5]. It is remarkable that nuclei as exotic as ^{48}Ni, *i.e.,* the mirror image of the double closed-shell nucleus ^{48}Ca, are now being studied!

The halo nuclei (or drip-line nuclei) may well play a central role in our understanding of the nuclear binding. Their typical structure is that of a tightly bound inner core with a few outer nucleons that are loosely attached to the core. Although these exotic nuclei are bound, their binary subsystems are not. For instance, the halo nucleus ^6He (^{11}Li) is presumably made of a ^4He (^9Li) core surrounded by a two-neutron halo. As a whole ^6He (^{11}Li) is bound, but its binary subsystems, *i.e.,* ^5He (^{10}Li) and the *di-neutron* are unbound. The pairing force between the valence nucleons is thus essential for the stability of the halo nuclei, and it is important to calculate it as accurately as we can.

So far, the halo nuclei have been calculated using empirical effective interactions, tuned to stable nuclei. The inherent density dependence of Skyrme-type forces [3,4] provides a reasonable means of extrapolating to the lower density regimes characteristic of nuclei far from stability. Yet, quite recently Kuo *et al.* [6] have suggested to study the drip-line nuclei from the first principles, *i.e.,* from the elementary nucleon-nucleon (NN) force, such as the Paris [7] and Bonn [8] interactions. Halo nucleons are separated rather far from the other nucleons in the "core nucleus", and the interaction among them should be derivable from the free NN interaction with small medium corrections.

Starting from a free NN interaction, a model-space effective interaction (V_{eff}) among the nucleons in the nuclear medium can be derived, using a G-matrix folded-diagram approach [9,10]. The major difficulty in such a microscopic effective interaction theory has been the treatment of the core polarization effect (CPE), in particular the higher-order core polarization diagrams. In ordinary nuclei, the valence nucleons are close to the nuclear

core, an example being the two *sd*-shell neutrons of ^{18}O residing adjacently to the ^{16}O core. Consequently, there is a strong valence-core coupling and therefore a large CPE. It is a formidable task to figure out in such a situation which G-matrix diagrams should be embodied in the $\hat{Q}$-box. The two leading terms are the well-known first-order G-matrix diagram and the second-order core polarization diagram G_{3p1h} [11]. Hjorth-Jensen *et al.* [12] have investigated the third-order $\hat{Q}$-box diagrams for the *sd* shell. They concluded that, after folding, the net effect on V_{eff} was a change of about $10-15\%$, as compared with the case when only the first- and second- order ones were considered. Higher and higher-order core polarization diagrams rapidly become prohibitively more difficult to deal with. Thus in practice one can only include some low-order diagrams for the calculation of the $\hat{Q}$-box. Besides, when there are disagreements between theory and experiment, one is not sure if they are due to the NN interaction or to the approximation adopted in solving the many-body problems (such as the neglecting of the higher-order core polarization diagrams). The environment in the halo nucleons is different and may be more promising, because they are located quite far away from the core. A schematic comparison between normal and halo nuclei is given in Fig. 1. A relatively weak CPE is expected for halo nucleons, and therefore an V_{eff} predominately governed by the free NN interaction. That is, V_{eff} should be in essence the bare G-matrix, which presently can be calculated to a high degree of accuracy. Hence the halo nuclei, besides having excitingly interesting and exotic properties, may furnish as well a much better testing ground for the fundamental NN interactions, than ordinary nuclei.

Motivated by the above scenario, we present in this letter a microscopic derivation of the V_{eff} for halo nucleons in ^6He and ^{11}Li, starting from the Paris and Bonn NN potentials and using a G-matrix folded-diagram approach [9,10]. The main steps in such a derivation are:

i) *Choice of the model space* P. An important criterion for selecting the model space P is that its overlap, with the physical states under consideration, should be as large as possible. For instance, the ^4He, i.e., the ^6He core, should remain essentially as an ordinary α-particle, with little perturbation from the distant halo nucleons. For the P space we shall use a closed $(0s_{1/2})^4$ core (α-particle) with the valence (halo) nucleons confined in the $0p$

shell. Yet the halo nucleons have a much larger r.m.s. radius than the core, and therefore an oscillator constant $\hbar\omega$ considerable smaller than that given by the empirical formula $\hbar\omega = 45A^{-1/3} - 25A^{-2/3}$ MeV (valid for ordinary nuclei). It would not be then feasible to reproduce both radii, using shell model wave functions with a common $\hbar\omega$. One may get past this difficulty by including several major shells in the one-frequency shell model (OFSM) calculation. But this would be very tedious. A convenient and physically appealing solution to this problem is to employ a two-frequency shell model (TFSM) for the description of halo nuclei, as suggested in Ref. [6]. Within the TFSM one uses oscillator wave functions with $\hbar\omega_{in}$ and $\hbar\omega_{out}$ for the core (inner) and the halo (outer) orbits, respectively. The notations b_{in} and b_{out} also will be used from now on, with $b^2 \equiv \hbar/m\omega$. In the present work b_{in} is fixed at 1.45 fm, while b_{out} is treated as a variation parameter (or generator coordinate). To assure the orthonormality, we have actually used b_{in} for all the $\ell = 0$ waves $(0s_{1/2}, 1s_{1/2}, \cdots)$ and b_{out} for waves with other ℓ values.

ii) *Evaluation of the model-space G-matrix.* For ordinary nuclei, the G-matrix can be calculated rather accurately with the method developed in Refs. [13,14]. We extend below this method to the halo nucleons in the context of the TFSM. For a general model-space P, we define the corresponding Brueckner G-matrix by the integral equation [14,15]

$$G(\omega) = V + VQ_2 \frac{1}{\omega - Q_2 T Q_2} Q_2 G(\omega),$$

where ω is an energy variable, Q_2 is a two-body Pauli exclusion operator, and T is the two-nucleon kinetic energy. Note that our G-matrix has orthogonalized plane-wave intermediate states. The exact solution of this G-matrix is $G = G_F + \Delta G$ [13,14], where G_F is the *free* G-matrix, and ΔG is the Pauli correction term

$$\Delta G(\omega) = -G_F(\omega)\frac{1}{e}P_2 \frac{1}{P_2[\frac{1}{e} + \frac{1}{e}G_F(\omega)\frac{1}{e}]P_2} P_2 \frac{1}{e} G_F(\omega),$$

with $e \equiv \omega - T$. The projection operator P_2, defined as $(1 - Q_2)$, will be discussed later. The basic ingredient for calculating the above G-matrix is the matrix elements of G_F within the P_2 space. This space contains all the two-particle states that must be excluded from

the intermediate states in G-matrix calculations. For ordinary nuclei, where the OFSM is used, the states excluded by the Pauli operator and those contained within the model space have a common length parameter b. For halo nuclei, where we use the TFSM, the situation is more complicated, as the wave functions for the excluded states and those within the model space have in general different length parameters b_{in} and b_{out}. Hence to calculate ΔG, we need the matrix elements of G_F in a $b_{in} - b_{out}$ mixed representation. This poses a technical difficulty because the transformations, from the c.m. coordinates to the laboratory coordinates for two-particle states with different oscillator lengths, are not as easy to perform as for one common oscillator length. We have adopted an expansion procedure to surmount this difficulty. Namely, we expand the oscillator wave functions with b_{in} in terms of those with b_{out}, or *vice versa*. When b_{in} and b_{out} are not too different from each other, this procedure is relatively effortless to carry out. Usually a high accuracy can be attained by including about 8 terms in the expansion. Still, the calculation of the two-frequency G-matrix is significantly more complicated than the ordinary one-frequency one. Another difficulty, in deriving the G-matrix for halo nuclei, is the treatment of its Pauli exclusion operator. As the halo nucleons are rather far from the core nucleons, the effect of Pauli blocking is expected to be small. But, to get a reliable result for a small effect, a very accurate procedure has to be employed. We write the projection operator Q_2 as

$$Q_2 = \sum_{all\ ab} Q(ab)|ab\rangle\langle ab|,$$

where $Q(ab) = 0$, if $b \leq n_1,\ a \leq n_3$, or $b \leq n_2,\ a \leq n_2$, or $b \leq n_3,\ a \leq n_1$, and $Q(ab) = 1$ otherwise. The boundary of $Q(ab)$ is specified by the orbital numbers (n_1, n_2, n_3). We denote the shell model orbits by numerals, starting from the bottom of the oscillator well: 1 for orbit $0s_{1/2}$, 2 for $0p_{3/2}, \cdots, 7$ for $0f_{7/2}$, and so on. n_1 and n_2 stand for the highest orbits of the closed core (Fermi sea) and of the chosen model space, respectively. For example, we consider ^4He as a closed core and all 6 orbits in the *sp* and *sd* shells are included in the model space. Then $n_1 = 1$ and $n_2 = 6$. As for the G-matrix intermediate states we consider only particle states (*i.e.,* states above the Fermi sea), n_3 in principle should be ∞ [14]. Still, in

practice this is not feasible, and n_3 has to be determined by an empirical procedure. Namely, we perform calculations with increasing values for n_3 until numerical results become stable. In Table 1, we display some representative results of our two-frequency G-matrix for the $\{0s0p\}$ model space, with $b_{in} = 1.45$ fm and $b_{out} = 2.0$ fm. The only approximation here is the finite n_3 truncation. A satisfactory n_3 convergence is attained for $n_3 = 21$, and this value is used here. It is worth noting that, although the halo nucleons are widely separated from the closed core, the Pauli correction term ΔG $(= G - G_F)$ is still quite significant.

iii) *Calculation of the irreducible diagrams for the vertex function $\hat{Q}$-boxes.* Once derived the G-matrix, we can calculate the irreducible vertex function $\hat{Q}$-box. Finally, the model-space energy-independent V_{eff} is evaluated in terms of the $\hat{Q}$-box folded-diagram series [9,10], following closely the procedures of Ref. [11].

Diagonal matrix elements of G, G_{3p1h} and V_{eff}, for the states $|(p_{3/2})^2; T = 1, J = 0\rangle$ and $|(p_{1/2})^2; T = 1, J = 0\rangle$, are shown in Fig. 2 as a function of b_{out}, for both the Paris and Bonn-A potentials. As we increase b_{out}, we are augmenting the average distance between the halo nucleons and the core and so reducing the coupling between them. For sufficiently large b_{out}, the total CPE must be small and it should be sufficiently accurately given by the second-order (lowest order) core polarization diagram alone. In fact, as b_{out} increases, the core polarization diagrams G_{3p1h} approach rapidly and monotonically to zero and become negligibly small at $b_{out} \cong 2.25$ fm. In our TFSM approach, we have assumed a fixed ^4He or ^9Li core, always described by $b_{in} = 1.45$ fm. Therefore the energy denominator for the diagram G_{3p1h} is fixed by the corresponding core and does not change with b_{out}. This means that the suppression of G_{3p1h} is entirely due to the weakening of the core-valence particle interaction. The behavior of the bare G-matrix and V_{eff} shown in Fig. 2 are also of interest. First, they are quite similar to each other. Second, while for the $p_{3/2}$ case, they become weaker as b_{out} increases, in the $p_{1/2}$ case they become stronger as b_{out} increases. Third, at large b_{out} the results given by the Paris and Bonn A potentials are practically identical. This is because their long-range parts do not differ much from each other.

To assess to which extent the nuclear model formulated above is reliably it is necessary

to compare our results with experiments. The valence or pairing interaction energy between the halo nucleons in ^6He is obtained from the odd-even mass difference [16]

$$E_p^{exp}(^6He) = -[\mathcal{B}(^6He) + \mathcal{B}(^4He) - 2\mathcal{B}(^5He)] = -2.77 \text{ MeV}.$$

To calculate this energy, we need to diagonalize the folded-diagram V_{eff} [11] in a $p_{3/2}$ and $p_{1/2}$ model space ($T = 1, J = 0$). In this way we get $E_p^{th} = -2.97$ MeV at $b_{out} = 2.25$ fm for the Paris potential. As the CPE is strongly suppressed for such a b_{out} value, this result almost entirely comes from the bare G-matrix. The ground-state wave function of ^6He is almost pure $(p_{3/2})^2$, with very little $(p_{1/2})^2$ admixture. Thus our E_p^{th} is also close to the diagonal G-matrix element shown in Fig. 2. As we have used a $p_{3/2} - p_{1/2}$ model space, our wave function for ^{11}Li has only one component (neutron orbits closed). Then the diagonal $(p_{1/2})^2(T = 1, J = 0)$ matrix element of V_{eff}, which is quite close to the unfolded value of Fig. 2 at $b_{out} = 2.25$ fm, is directly comparable to the pairing energy for ^{11}Li. From the masses of ^{11}Li, ^{10}Li and ^9Li [16], we get $E_p^{exp} = -1.14$ MeV, while our result is $E_p^{th} = -0.81$ MeV at $b_{out} = 2.25$ fm for the Paris potential. This discrepancy could be pointing out that some physics is still missing in our description of the valence ^{11}Li neutrons. It is very likely that they should not be entirely confined to the p shell, but a larger space, such as $\{0p_{1/2}0d1s\}$, is probable needed.

In passing, we mention that the above $b_{out} = 2.25$ fm is a reasonable choice. Recall that we have fixed $b_{in} = 1.45$ fm. With these values of b_{in} and b_{out}, and assuming a pure s^4p^n wave function, we get that $R^{th}(^6He) = 2.51$ fm, in good agreement with the empirical value $R^{exp}(^6He) = 2.57 \pm 0.1$ fm [17]; similarly, $R^{th}(^{11}Li) = 3.03$ fm while $R^{exp}(^{11}Li) = 3.1 \pm 0.1$ fm [17].

We have also calculated the valence interaction energy for ^6Li using a similar folded-diagram procedure in the $p_{3/2} - p_{1/2}$ space. From the empirical masses of ^6Li, ^5Li, ^5He and ^4He [16], we obtain $E_v^{exp} = -6.56$ MeV. (This number was incorrectly given as -3.55 MeV in Ref. [6].) Our result is $E_v^{th} = -6.64$ MeV for the Paris potential, if we use $b_{out} = 1.75$ and $b_{in} = 1.45$ fm. It is of interest to stress that ^6Li is *not* a halo nucleus, according to

our calculation, in the sense that there is no need to employ a very large b_{out} for its valence nucleons.

In summary, we have derived the effective interaction for the valence nucleons in halo nuclei, starting from realistic NN interactions. Our preliminary results are encouraging. We have employed a two-frequency shell model approach, to give a good spatial description for both the core nucleons and the halo nucleons. While keeping the inner length parameter b_{in} fixed, we gauge the spatial extension of the halo nucleons by varying the outer length parameter b_{out}. In this way we have explicitly proved that the core polarization effect is strongly suppressed at large b_{out} values, as required by the large empirical r.m.s. radii of halo nuclei. Ergo, *the effective interaction between the halo nucleons is predominantly given by the bare G-matrix alone*, in accord with our expectations. The Pauli blocking effect on the G-matrix has been found to be very important, and it can be calculated quite accurately as we have demonstrated. Thus it appears that one can derive the effective interaction for halo nuclei much more accurately than for ordinary nuclei. We enthusiastically believe that the halo nuclei, which have already greatly enhanced our knowledge about nuclei, may in addition provide a more accurate testing ground for the fundamental NN interaction, than the ordinary nuclei.

ACKNOWLEDGMENTS

This work is supported in part by the USDOE Grant DE-FG02-88ER40388, by the NSF Grant and by the Fundación Antorchas (Argentina). One of us (T.T.S. Kuo) is grateful for the warm hospitality extended to him while visiting the Universidad Nacional de La Plata.

REFERENCES

[1] S.M. Austin and G.F. Bertsch, Scientific American June 1995 p62.

[2] J.S. Al-Khalili, Physics World June 1996 p33.

[3] W. Nazarewicz *et al.*, Phys. Rev. **C53** 740 (1996).

[4] I. Hamamoto, H. Sagawa, and X.L. Zhang, Phys. Rev. **C53** 765 (1996); I. Hamamoto and H. Sagawa, Phys. Rev. **C53** 1492 (1996).

[5] R.D. Page *et al.*, Phys. Rev. **C53** 660 (1996).

[6] T.T.S. Kuo, H. Muether and Azimi-Nilli, to be published in *Festschrift commemorating G.E. Brown's 70th birthday* (North-Holland Elsevier 1996).

[7] M. Lacombe *et al.*, Phys. Rev. **C21** 861 (1980).

[8] R. Machleidt, Adv. Nucl. Phys. **19** (1989) 189.

[9] T.T.S. Kuo and E. Osnes, *Lecture Notes in Physics* **Vol.364** (Springer-Verlag 1990) p. 1.

[10] T.T.S. Kuo, E. Krmpotić, K. Suzuki and R. Okamoto, Nucl. Phys. **A582**, (1995) 205.

[11] J. Shurpin, T.T.S. Kuo, and D. Strottman, Nucl. Phys. **A408**, 310 (1983).

[12] M. Hjorth-Jensen, T.T.S. Kuo and E. Osnes, Phys. Rep. **261** (1995) 126.

[13] S.F. Tsai and T.T.S. Kuo, Phys. Lett. **B39** 427 (1972).

[14] E.M. Krenciglowa, C.L. Kung, T.T.S. Kuo and E. Osnes, Ann. Phys. (N.Y.) **101**, 154 (1976).

[15] H. Müther and P. Sauer, in *Computational Nuclear Physics 2*, ed. by K. Langanke, J.A. Maruhn and S. Koonin, Springer-Verlag 1992, p. 30.

[16] J.K. Tuli (editor), *Nuclear Wallet Cards*, National Nuclear Data Center, Brookhaven

National Laboratory (1995).

[17] M.V. Zhukov *et al.*, Phys. Rep. **231**, 151 (1993), and Refs. therein.

TABLES

TABLE I. Dependence of the two-frequency G-matrix on the choice of n_3. Listed are the matrix element $\langle (0p_{3/2})^2; TJ|G(\omega)|(0p_{3/2})^2; TJ\rangle$ (in MeV), calculated for the Paris potential and three different values of ω (in MeV), with $TJ = 01$ (upper panel) and with $TJ = 10$ (lower panel). We have used $b_{in} = 1.45$ and $b_{out} = 2.0$ fm for the length parameters, and $n_1 = 1$ and $n_2 = 6$ for the exclusion operator. The first row in each group (F) denotes the free G-matrix.

n_3	$\omega = -5$	$\omega = -10$	$\omega = -20$
F	-6.896	-4.530	-3.155
6	-2.218	-2.115	-1.885
15	-2.217	-2.114	-1.882
21	-2.217	-2.114	-1.882
F	-4.422	-3.933	-3.480
6	-2.768	-2.748	-2.701
15	-2.761	-2.744	-2.698
21	-2.761	-2.744	-2.698

Figure Captions

Fig. 1 Comparison of core polarization in ordinary and halo nuclei.

Fig. 2 Diagonal matrix elements of G_{3p1h} (dotted lines), G (dashed lines) and V_{eff} (full lines) for the states $|(p_{3/2})^2; T = 1, J = 0\rangle$ (upper panel) and $|(p_{1/2})^2; T = 1, J = 0\rangle$ (lower panel) as a function of b_{out}; calculations done with Paris and Bonn-A potentials are shown by open and solid symbols, respectively. The G-matrix curves are for $\omega = -5$ MeV and Pauli exclusion operator with $(n_1, n_2, n_3) = (1, 3, 21)$.

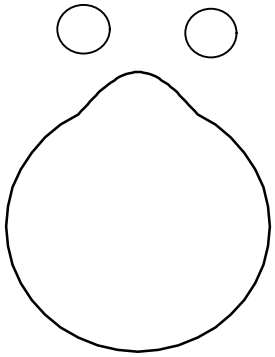

Normal Nucleus

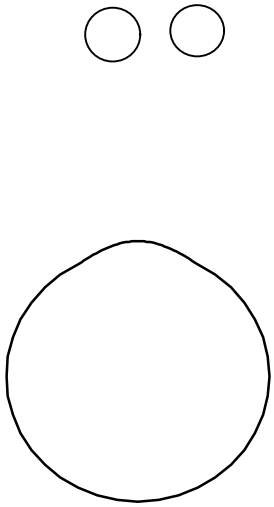

Halo Nucleus

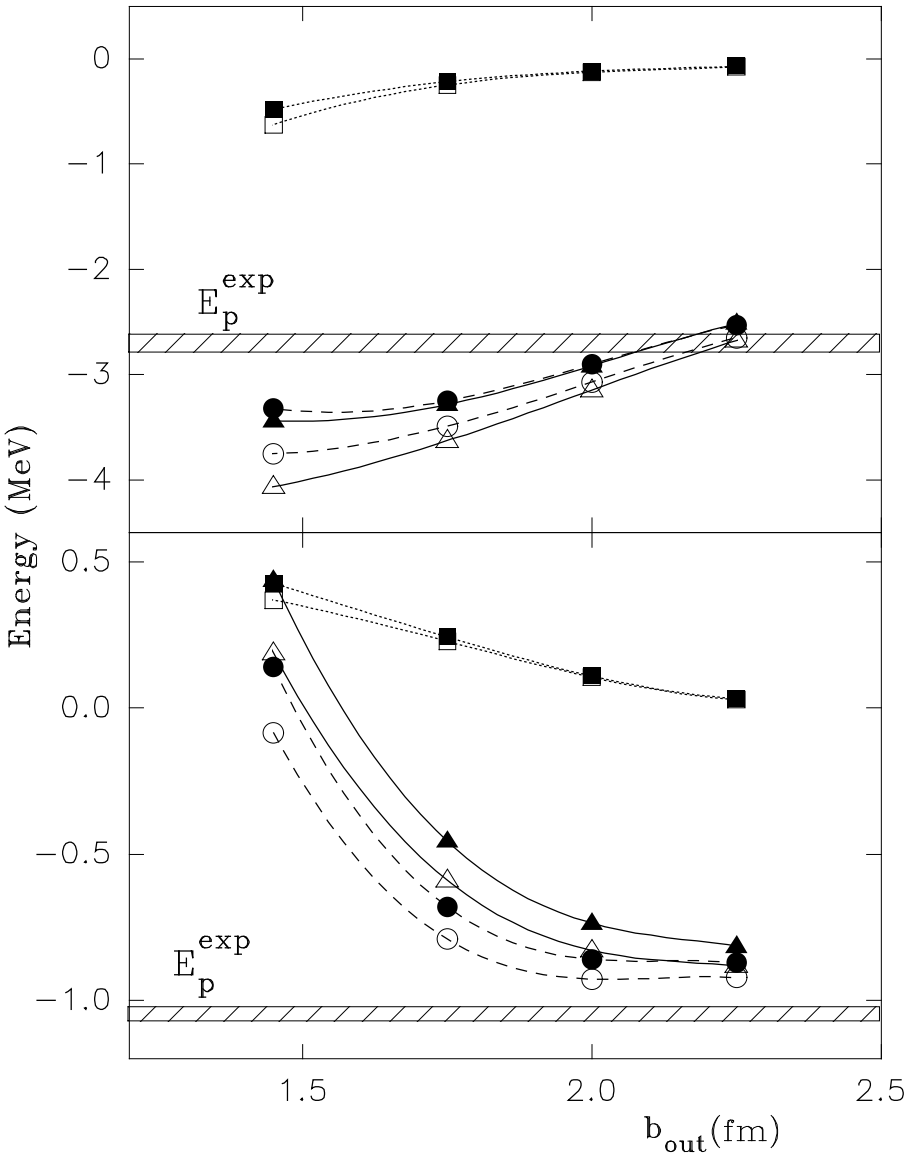
0
−1
−2
−3
−4
0.5
0.0
−0.5
−1.0
Energy (MeV)
E_p^{exp}
E_p^{exp}
1.5
2.0
2.5
b_{out}(fm)